$[Au^{I}(CN)_2]$-Armed $[Fe^{III}_2Fe^{II}_2]$ Square Complex Showing Unusual Spin-Crossover Behavior Due to a Symmetry-Breaking Phase Transition

Maolin You,[†,‡] Dong Shao,[†] Yi-Fei Deng,[†,*] Jiong Yang,[†] Nian-Tao Yao,[#] Yin-Shan Meng,[#] Liviu Ungur,[‡] and Yuan-Zhu Zhang[†,*]

[†] Department of Chemistry, Southern University of Science and Technology (SUSTech), Shenzhen, 518055, China.

[‡] Department of Chemistry, National University of Singapore, Science Drive 3, Singapore, 117543, Singapore.

[#] State Key Laboratory of Fine Chemicals, Dalian University of Technology, 2 Linggong Rd., Dalian, 116024, China.

E-mail: dengyf@sustech.edu.cn; zhangyz@sustech.edu.cn

Experimental Section

Materials. $[NEt_4][(Tp^{*Me})Fe^{III}(CN)_3]$, and di(1*H*-pyrazol-1-yl)di(pyridin-2-yl)methane (L) were prepared based on the previous literatures.[1,2] All other chemicals and solvents (reagent grade) were commercially available and used without further purification.

Caution. *Although no problem was encountered during this work, cyanides are highly toxic. Thus, these materials should be handled in small quantities and with great caution.*

Physical Measurements. Elemental analysis for C, H, and N was performed on an Elementar Vario EL Cube elemental analyzer. Variable-temperature Infrared (IR) spectra were collected in the range 4000 - 600 cm^{-1} on a Bruker Tensor II spectrophotometer with a Specac Golden Gate low temperature ATR accessory (Attenuated Total Reflectance method, UK). Specifically, a small amount of finely ground solid sample of **1**·**2Et$_2$O** (~3 mg) was placed on the sample holder for the IR measurement, while the spectra data of **1** was in situ recorded after heating the sample of **1**·**2Et$_2$O** at 400 K for 10 mins. Powder X-ray diffraction (PXRD) data were recorded on a Rigaku Smartlab X-ray diffractometer with Cu Kα radiation (45 kV, 200 mA) between 5 and 50° (2θ). Thermogravimetric analysis (TGA) was carried out under an argon atmosphere at 3 K/min using a METTLER-TOLEDO TG2 instrument. Differential scanning calorimetry (DSC) measurements were recorded using a TA Instruments Discovery DSC2500 (USA) with a temperature sweep rate of 2 K/min. Magnetic measurements were performed on a Quantum Design SQUID MPMS3 magnetometer on the microcrystals of fresh sample of **1**·**2Et$_2$O**. Diamagnetic corrections were calculated from Pascal constants and applied to all the constituent atoms and sample holder.[3] The temperature-dependent ac (alternate current) dielectric permittivity measurements were performed on Quantum Design PPMS–9 with KEYSIGHT E4980AL under the applied voltage of 2.0 V in the temperature range of 100-400 K. For the dielectric experiment, a pellet was made from the sample of **1** under a pressure of about 8 MPa, which was released during the measurement. The pressed pellet was then attached on the electrodes by using silver conducting glue for the dielectric study.

Synthesis of $[\{(Tp^{*Me})Fe^{III}(CN)_3\}\{Fe^{II}(L)\}\{Au(CN)_2\}]_2$·2Et$_2$O (1·2Et$_2$O)

Treatment of $Fe(OTf)_2$ (0.025 mmol, 8.8 mg) and $[NEt_4][(Tp^{*Me})Fe^{III}(CN)_3]$ (0.025 mmol, 18.8 mg) in acetonitrile (2 mL) for 10 minutes, followed by dropwise addition of an acetonitrile solution (1 mL) of the ligand L (0.025 mmol, 7.5 mg) afforded a dark red solution, which was continuously

stirred for 20 minutes at room temperature before adding $K[Au(CN)_2]$ (0.025 mmol, 7.3 mg) in methanol (1 mL). The resulted mixture was stirred for another 5 minutes and then filtered. The filtrate was layered with diethyl ether (Et_2O), and dark red block-like single crystals were collected after two weeks. Yield: 25 mg, 43.3 %. Anal. Calcd (%) (found) for $C_{88}H_{104}B_2Au_2Fe_4N_{34}O_2$: C, 45.77 (45.69); H, 4.54 (4.61); N, 20.62 (20.52). The desolvated phase **1** was realized by heating sample **1** $\cdot$**2Et$_2$O** at 400 K for 10 mins. Anal. Calcd (%) (found) for $C_{80}H_{84}B_2Au_2Fe_4N_{34}$ (**1**): C, 44.47 (44.36); H, 3.92 (3.80); N, 22.04 (21.91).

The desolvated crystals (**1**) for X-ray diffraction were prepared by slowly heating the fresh sample of **1** $\cdot$**2Et$_2$O** from room temperature to 400 K via a programmed temperature control in the oven. After cooling to room temperature, the annealed crystals were obtained, which were used for SCXRD measurements at 350, 300 and 100 K, respectively. As a result, the crystallographic data at 350 K is solvent free while those at 300 and 100 K suggest the presence of a few lattice water molecules (about 0.25 equiv H_2O per asymmetry unit), most likely attributed to the water re-absorption during the cooling process in the oven. However, it is quite difficult to avoid that during the desolvation process in the air. The *in situ* desolvation via the X-ray diffractometer may be helpful but the crystal samples would lose their crystallinity when heating to 400 K in this way.

X-ray Diffraction. Single crystal X-ray diffraction (SCXRD) data for both **1** $\cdot$**2Et$_2$O** (100, 300 and 350 K), and **1** (100, 300, and 350 K) were collected on a Bruker D8 VENTURE diffractometer with graphite monochromated Mo Kα radiation (λ = 0.71073 Å). Lorentz/polarization corrections were applied during data reduction and the structures were solved by the direct method (SHELXL-2014).[4] Refinements were performed by full-matrix least squares (SHELXL-2014) on F^2 and empirical absorption corrections (SADABS) were applied.[5] Anisotropic thermal parameters were used for the non-hydrogen atoms. Hydrogen atoms were added geometrically and refined using a riding model. Weighted R factors (wR) and all the goodness-of-fit (S) values are based on F^2; conventional R factors (R) are based on F, with F set to zero for negative F^2. CCDC 2086214 (**1** $\cdot$**2Et$_2$O**_100 K), 2086215 (**1** $\cdot$**2Et$_2$O**_300 K), 2086216 (**1** $\cdot$**2Et$_2$O**_350 K), 2086217 (**1**_100 K), 2086218 (**1**_300 K), and 2086219 (**1**_350 K) contain the crystallographic data that can be obtained via www.ccdc.cam.ac.uk/conts/retrieving.html (or from the Cambridge Crystallographic Data Centre, 12, Union Road, Cambridge CB21EZ, UK; fax: (+44) 1223-336-033; or deposit@ccdc.cam.ac.uk).

References

(1) Zhang, Y.; Mallik, U. P.; Rath, N.; Yee, G. T.; Clérac, R.; Holmes, S. M., A cyano-based octanuclear $\{Fe^{III}_4Ni^{II}_4\}$ single-molecule magnet. *Chem. Commun.* **2010**, *46*, 4953-4955.

(2) Park, J.-E.; Kang, S. K.; Woo, J. O.; Son, K.-s., Highly active chromium(III) complexes based on tridentate pyrazolyl pyridyl ligands for ethylene polymerization and oligomerization. *Dalton Trans.* **2015**, *44*, 9964-9969.

(3) Bain, G. A.; Berry, J. F., Diamagnetic Corrections and Pascal's Constants. *J. Chem. Educ.* **2008**, *85*, 532-536.

(4) Sheldrick, G. M. *SHELXL-2014*, Program for the solution of crystal structures. University of Göttingen, Göttingen, Germany, **2014**.

(5) (a) Sheldrick, G. M. *SHELXL-2014*, Program for Crystal Structure Refinement. University of Göttingen, Göttingen, Germany, **2014**; (b) Sheldrick, G. M. *SADABS*, v.2.01, Bruker/Siemens Area Detector Absorption Correction Program. Bruker AXS: Madison, Wisconism, **1998**.

Table S1. Crystallographic data for **1**·2Et_2O.

	1·2Et_2O		
Formula	$C_{88}H_{104}B_2Au_2Fe_4N_{34}O_2$		
M_w/g mol^{-1}	2309.00		
T / K	100	300	350
Crystal system	Monoclinic	Monoclinic	Monoclinic
Space group	*C2/c*	*C2/c*	*C2/c*
a, Å	30.7214(17)	31.053(3)	31.164(7)
b, Å	16.0888(11)	16.3423(14)	16.380(4)
c, Å	19.9451(10)	20.1266(13)	20.260(4)
α, deg	90	90	90
β, deg	102.710(2)	102.922(3)	102.780(8)
γ, deg	90	90	90
V, Å^3	9616.7(10)	9955.0(13)	10086(4)
Z	4	4	4
D_{cal}/g cm^{-3}	1.595	1.541	1.521
2θ range/^{o}	4.8 to 55.05	4.414 to 50.084	4.392 to 51.046
completeness	99.9 %	98.5 %	98.9 %
GOF	1.125	1.033	1.006
R indices	R_1 = 0.0570	R_1 = 0.0603	R_1 = 0.0469
[$I > 2\delta(I)$][a,b]	wR_2 = 0.1371	wR_2 = 0.1464	wR_2 = 0.1122
R indices	R_1 = 0.0675	R_1 = 0.0960	R_1 = 0.1017
(all data)	wR_2 = 0.1426	wR_2 = 0.1688	wR_2 = 0.1413

[a] $R_1 = \sum \| F_o | - | F_c \| / [\sum |F_o|]$ [b] $wR_2 = \left[\sum [w(F_o^2 - F_c^2)^2] / \sum [w(F_o^2)^2]\right]^{1/2}$ $w = 1/\sigma^2(F_o^2) + (aP)^2 + bP$ where $P = [\max(0 \text{ or } F_o^2) + 2(F_c^2)]/3$

Table S2. Crystallographic data for **1**.

	1		
Formula	$C_{80}H_{85}B_2Au_2Fe_4N_{34}O_{0.5}$		$C_{80}H_{84}Au_2B_2Fe_4N_{34}$
M_w /g mol^{-1}	2169.77		2160.76
T / K	100	300	350
Crystal system	Monoclinic	Monoclinic	Monoclinic
Space group	*C2/c*	*C2/c*	*C2/c*
a, Å	53.3227(16)	54.221(7)	29.135(6)
b, Å	31.1517(9)	31.235(4)	15.381(3)
c, Å	21.2752(6)	21.600(3)	21.021(4)
α, deg	90	90	90
β, deg	101.2410(10)	101.269(4)	103.402(5)
γ, deg	90	90	90
V, Å^3	34662.1(17)	35876(7)	9164(3)
Z	16	16	4
D_{cal}/g cm^{-3}	1.663	1.607	1.566
2θ range/^{o}	4.476 to 55.11	4.49 to 50.188	4.722 to 33.082
completeness	99.9 %	99.4 %	100 %
GOF	1.056	1.066	1.133
R indices	R_1 = 0.0692	R_1 = 0.0662	R_1 = 0.0520
[$I > 2\delta(I)$][a,b]	wR_2 = 0.1418	wR_2 = 0.1230	wR_2 = 0.1319
R indices	R_1 = 0.1487	R_1 = 0.1805	R_1 = 0.0648
(all data)	wR_2 = 0.1833	wR_2 = 0.1692	wR_2 = 0.1495

[a] $R_1 = \sum \| F_o | - | F_c \| / [\sum |F_o|]$ [b] $wR_2 = \left[\sum [w(F_o^2 - F_c^2)^2] / \sum [w(F_o^2)^2]\right]^{1/2}$ $w = 1/\sigma^2(F_o^2) + (aP)^2 + bP$ where $P = [\max(0 \text{ or } F_o^2) + 2(F_c^2)]/3$

Table S3. Selected bond lengths (Å) for **1**·2Et_2O at 100, 300 and 350 K.

parameter	100 K	300 K	350 K
Fe1-N1	1.932(5)	1.959(6)	1.990(5)
Fe1-N2	1.935(5)	1.957(7)	1.997(5)
Fe1-N3	1.949(5)	1.961(8)	2.021(7)
Fe1-N4	1.981(3)	1.990(4)	2.052(5)
Fe1-N5	2.005(5)	2.053(7)	2.122(5)
Fe1-N6	1.923(5)	1.924(5)	2.003(5)
Fe2-N8	1.996(5)	1.996(6)	2.001(5)
Fe2-N9	2.018(5)	2.008(7)	1.997(5)
Fe2-N10	2.000(5)	1.996(7)	2.001(5)
Fe2-C1	1.918(6)	1.915(7)	1.912(6)
Fe2-C2	1.914(6)	1.904(8)	1.897(6)
Fe2-C3	1.920(7)	1.914(11)	1.906(9)

Table S4. Selected bond lengths (Å) for **1** at 100, 300 and 350 K.

parameter	100 K	300 K	350 K
Fe1-N1	1.943(6)	2.065(9)	2.110(18)
Fe1-N2	1.970(7)	2.066(10)	2.044(18)
Fe1-N4	1.961(6)	2.091(11)	2.127(19)
Fe1-N17	1.987(6)	2.234(9)	2.256(17)
Fe1-N18	2.002(5)	2.236(10)	2.270(16)
Fe1-N19	1.920(7)	2.114(10)	2.082(16)
Fe2-N38	2.006(6)	2.003(9)	2.022(16)
Fe2-N62	1.991(7)	1.994(8)	1.992(15)
Fe2-N65	1.995(5)	2.009(8)	1.985(15)
Fe2-C1	1.945(7)	1.924(11)	1.85(2)
Fe2-C2	1.942(8)	1.931(13)	1.90(2)
Fe2-C3	1.904(7)	1.935(12)	1.90(2)
Fe3-N6	1.953(7)	1.982(10)	
Fe3-N9	1.930(6)	1.968(9)	
Fe3-N11	1.930(7)	1.958(11)	
Fe3-N20	1.990(7)	2.061(8)	
Fe3-N21	2.007(6)	2.067(11)	
Fe3-N22	1.911(7)	1.955(10)	
Fe4-N42	2.008(7)	2.003(8)	
Fe4-N43	1.994(6)	2.009(9)	
Fe4-N48	1.992(6)	2.000(8)	
Fe4-C5	1.923(7)	1.930(10)	
Fe4-C6	1.929(8)	1.931(12)	
Fe4-C7	1.922(8)	1.905(11)	
Fe5-N5	1.953(6)	1.968(8)	
Fe5-N8	1.941(7)	1.948(10)	
Fe5-N12	1.919(5)	1.925(9)	
Fe5-N23	1.939(7)	1.967(9)	
Fe5-N24	1.987(6)	2.007(8)	
Fe5-N25	1.939(7)	1.949(9)	
Fe6-N52	1.995(6)	1.997(8)	
Fe6-N55	2.007(7)	1.996(8)	
Fe6-N63	1.985(6)	1.992(9)	
Fe6-C8	1.909(9)	1.921(13)	
Fe6-C9	1.932(8)	1.925(11)	
Fe6-C10	1.928(10)	1.916(13)	
Fe7-N13	1.928(6)	1.942(10)	
Fe7-N14	1.950(6)	1.948(8)	
Fe7-N16	1.960(5)	1.934(9)	
Fe7-N26	1.947(6)	1.963(8)	
Fe7-N27	1.984(6)	2.002(8)	

Fe7-N28	1.949(6)	1.965(9)
Fe8-N32	1.986(6)	1.998(8)
Fe8-N54	1.996(6)	1.996(9)
Fe8-N67	1.993(6)	1.992(9)
Fe8-C13	1.910(8)	1.898(12)
Fe8-C14	1.937(7)	1.928(11)
Fe8-C15	1.915(8)	1.911(14)

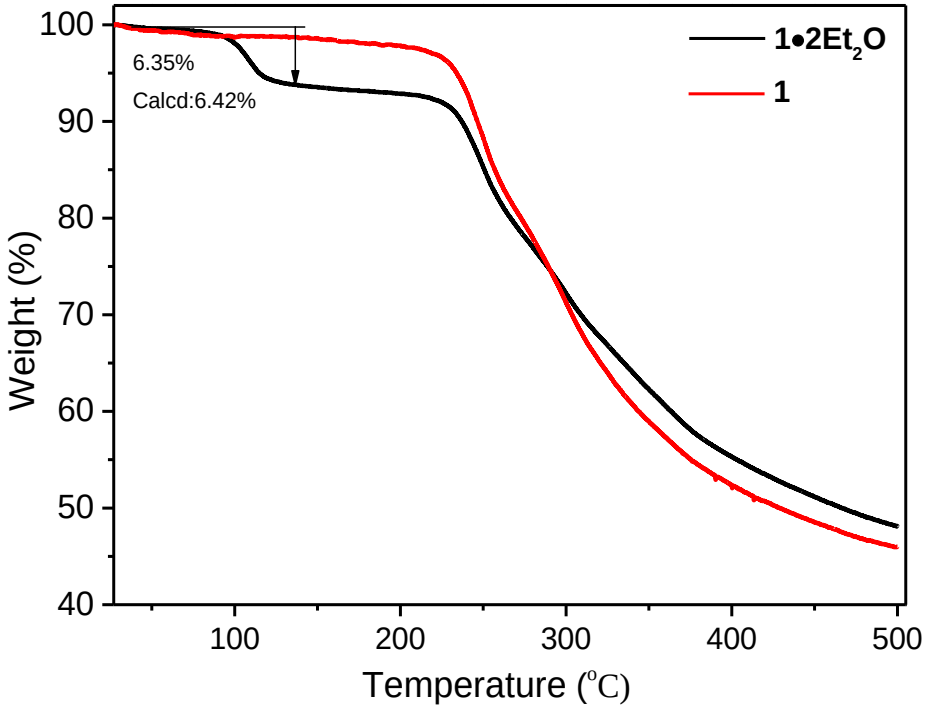

Figure S1. TGA curves of **1**·**2Et$_2$O** and **1** at a rate of 3 °C/min under an argon atmosphere.

Notably, a very small drop (about 0.8%) is observed for **1** below 100 °C, which is in consistent with the abovementioned water re-absorption during the desolvation process. However, it is difficult to accurately quantify this value because the weight proportion for this water molecule is only 0.41% from the crystallographic data.

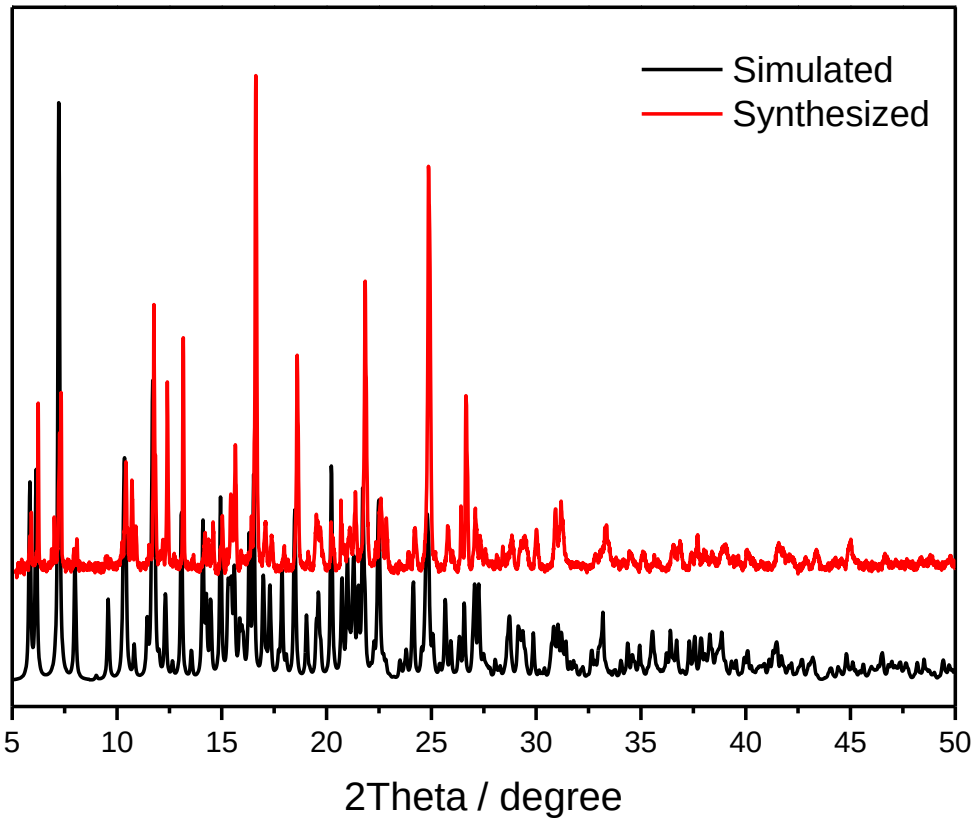

Figure S2. The room temperature PXRD pattern of **1 2Et$_2$O** (red) and the simulated spectra from single crystal data at 300 K (black).

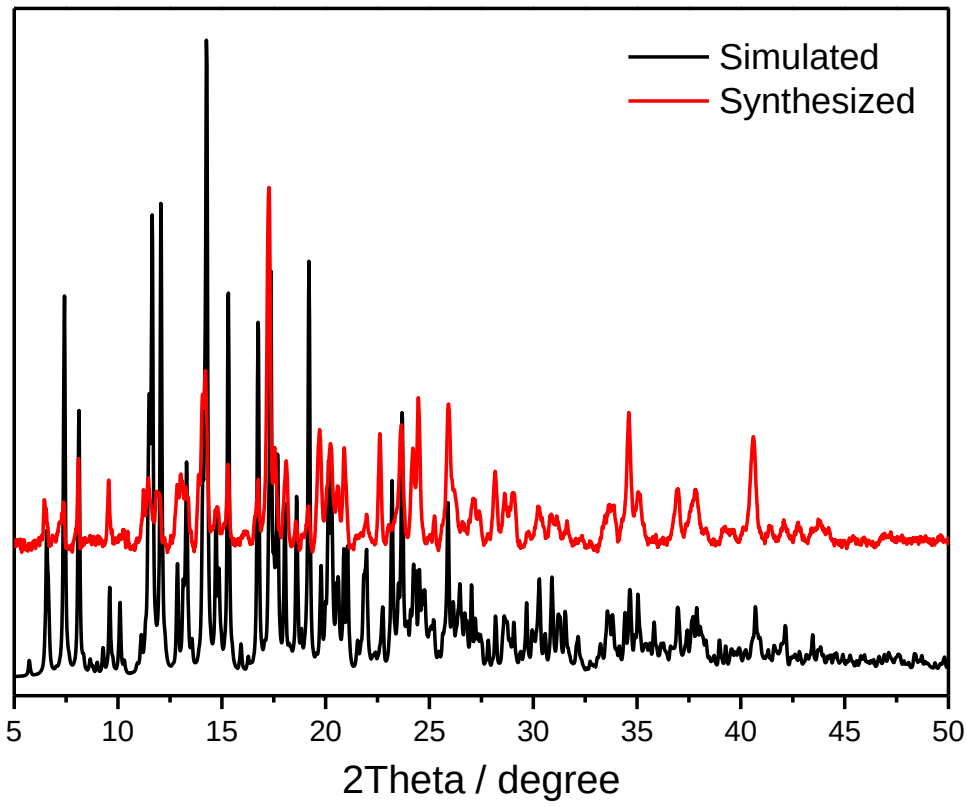

Figure S3. The room temperature PXRD pattern of **1** (red) and the simulated spectra from single crystal data at 300 K (black).

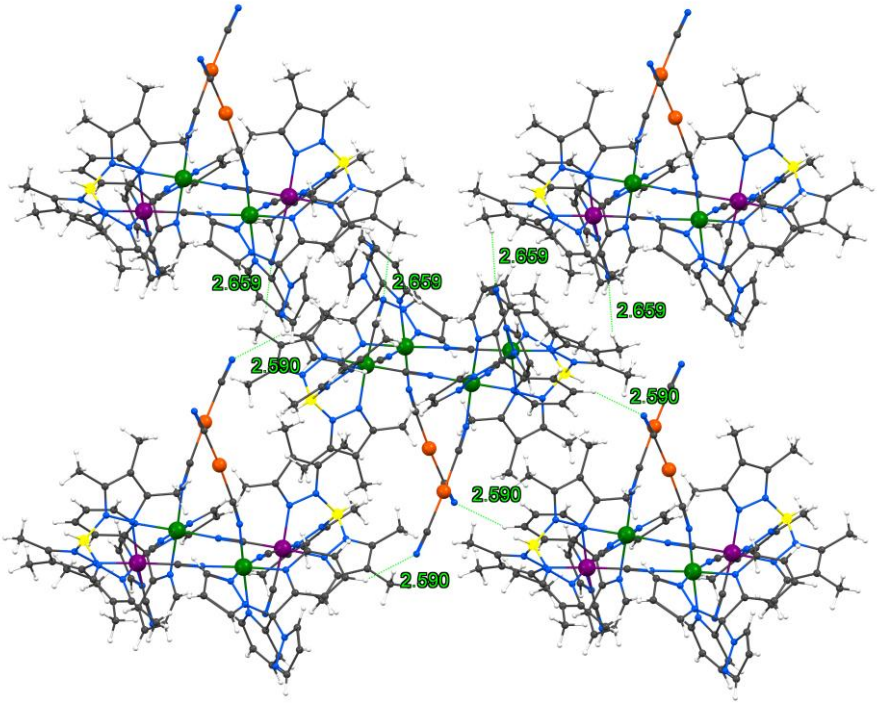

Figure S4. The packing structure of **1 2Et$_2$O** at 350 K showing intermolecular C-H···N interactions (2.590(1), 2.659(6) Å). The lattice solvent molecules are omitted for clarity. Color codes: Fe^{II}, green; Fe^{III}, purple; Au, orange; C, grey; N, Blue; B, yellow; H, pale grey.

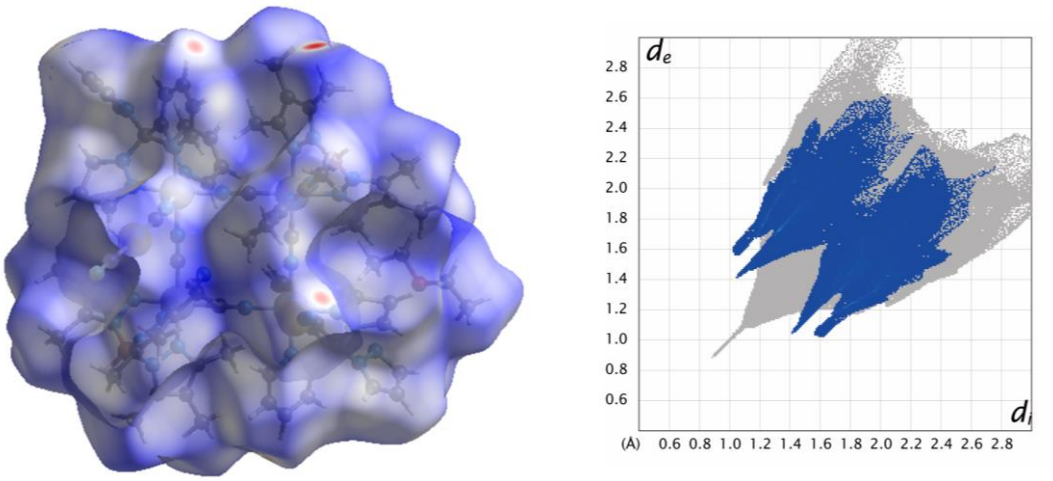

Figure S5. Hirshfeld surface mapped with d_{norm} (right), and 2D fingerprint plots of C-H···N interactions (left) for **1 2Et$_2$O** at 350 K.

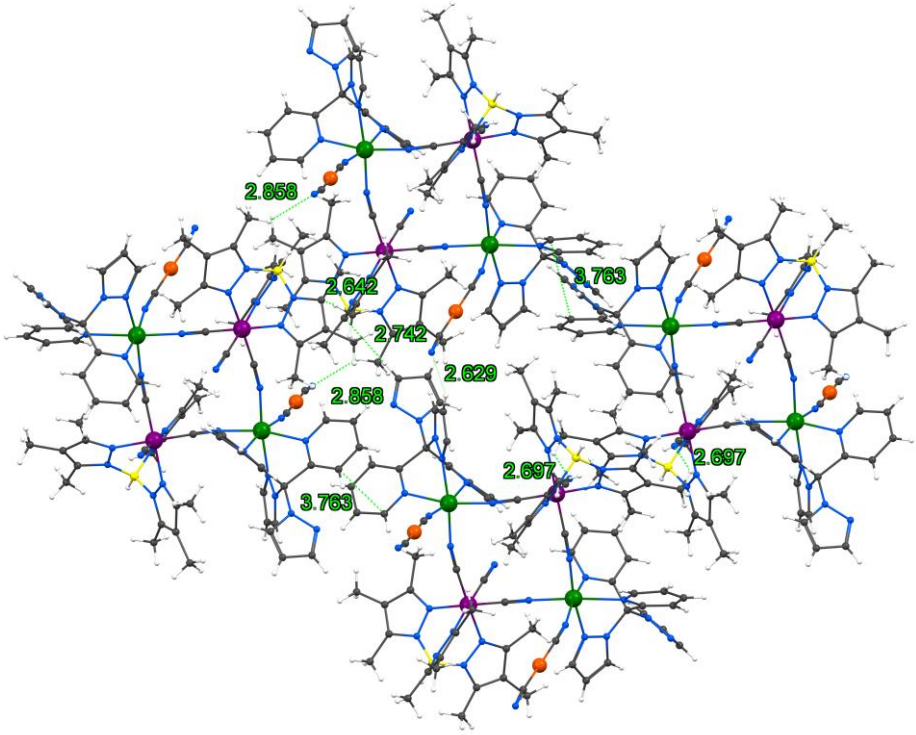

Figure S6. The packing structure of **1** at 350 K showing intermolecular C-H···N (2.629(2), 2.697(2), 2.858(1) Å), C-H···π (2.642(4), 2.742(2) Å) and π···π (3.760(1) Å) couplings. Color codes: Fe^{II}, green; Fe^{III}, purple; Au, orange; C, grey; N, Blue; B, yellow; H, pale grey.

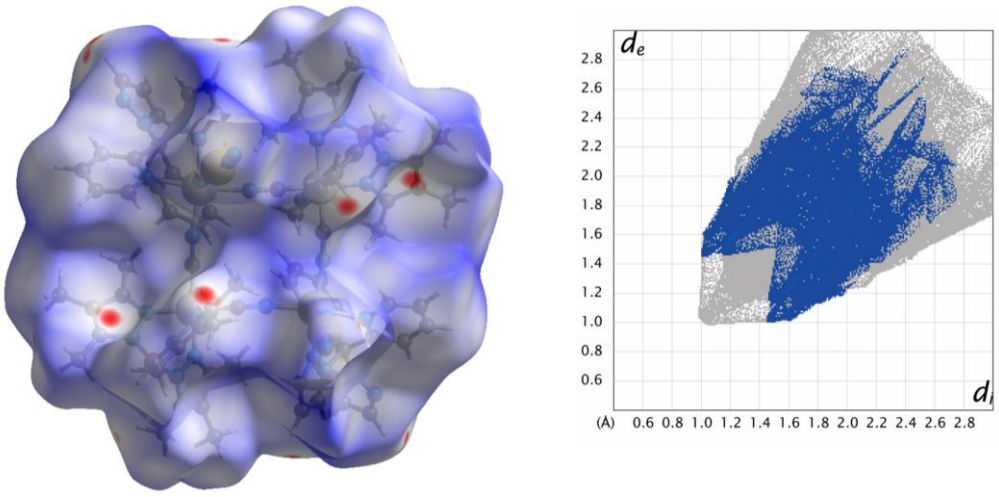

Figure S7. Hirshfeld surface mapped with d_{norm} (right), and 2D fingerprint plots of C-H···N interactions (left) for **1** at 350 K.

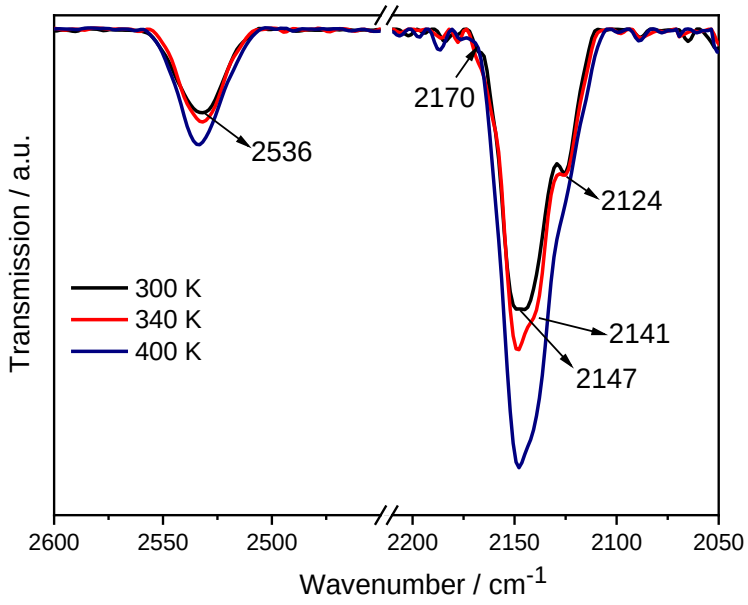

Figure S8. Variable temperature solid state infrared spectra for **1** $\cdot 2Et_2O$.

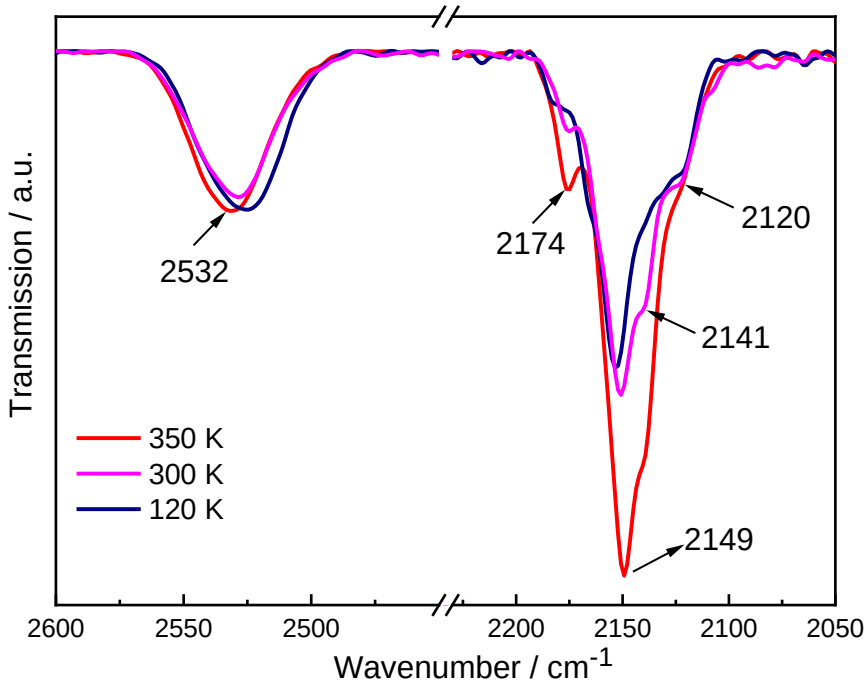

Figure S9. Variable temperature solid state infrared spectra for **1**.

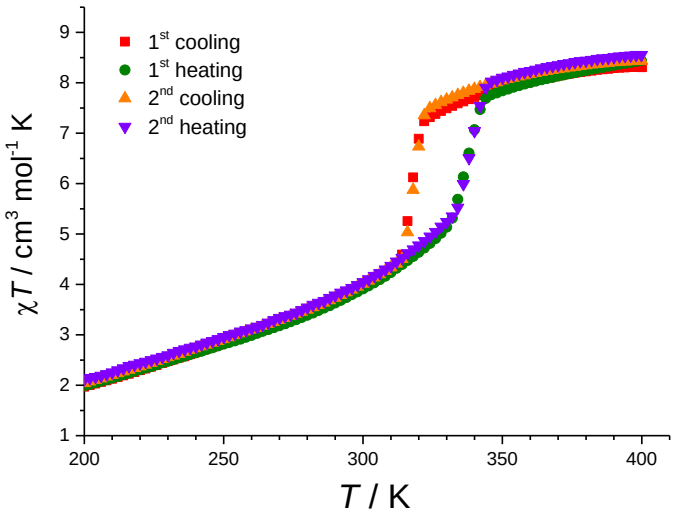

Figure S10. Two cycles of χT vs. T plots for **1** in sweep mode scanning at 200-410 K (2 K/min).

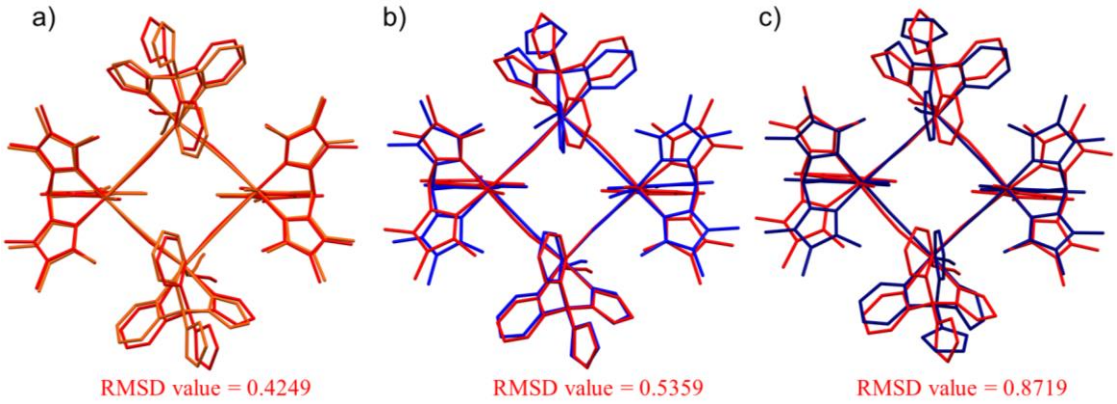

Figure S11. Molecular overlays of **1** at 350 and 300 K. Squares B (a), C (b), D (c) at 350 K are colored in red, those at 300 K are colored in orange, blue and navy, respectively.

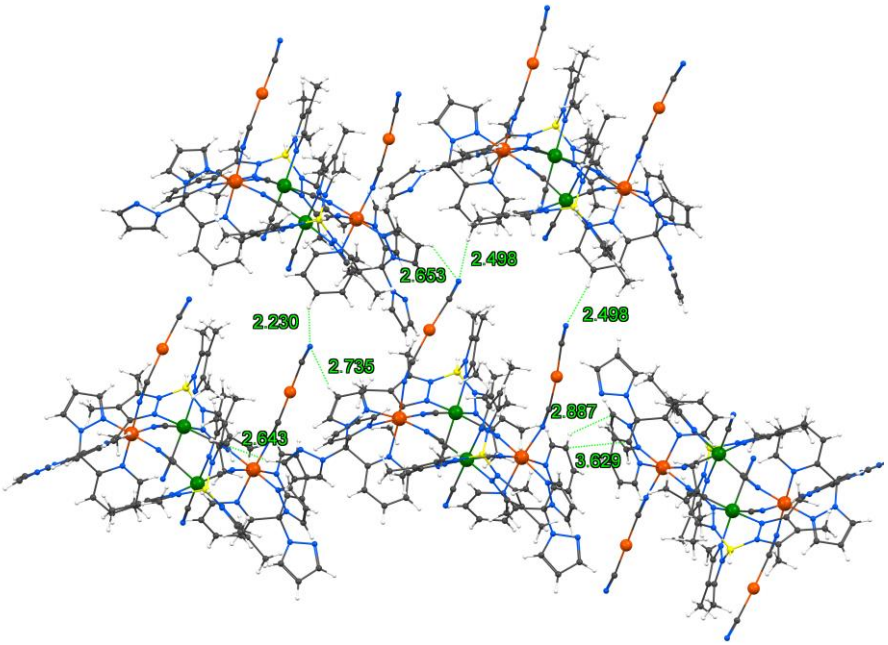

Figure S12. The packing structure of **1** at 300 K showing intermolecular C-H···N (2.230(2), 2.498(1), 2.653(2), 2.735(2) Å), C-H···π (2.643(2), 2.887(1) Å) and π···π (3.629(1) Å) couplings. Color codes: Fe^{II}, green; Fe^{III}, purple; Au, orange; C, grey; N, Blue; B, yellow; H, pale grey.

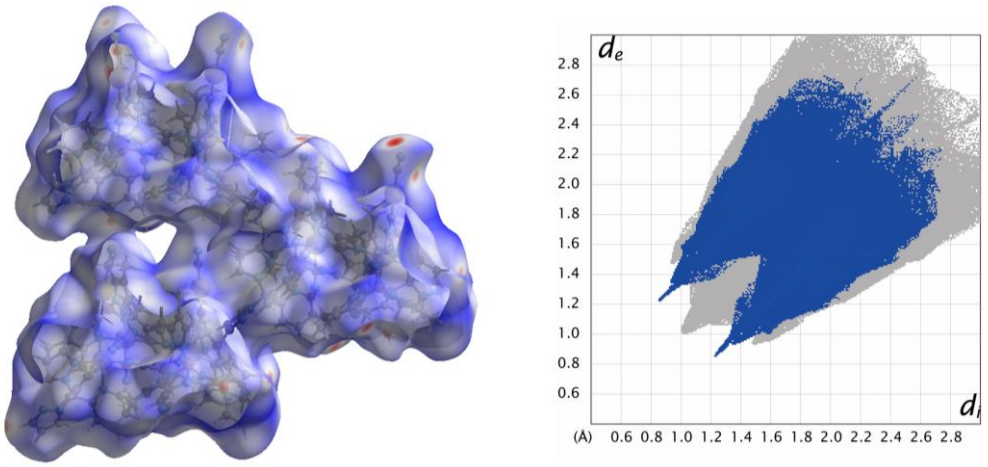

Figure S13. Hirshfeld surface mapped with d_{norm} (right), and 2D fingerprint plots of C-H ··N interactions (left) for **1** at 300 K.

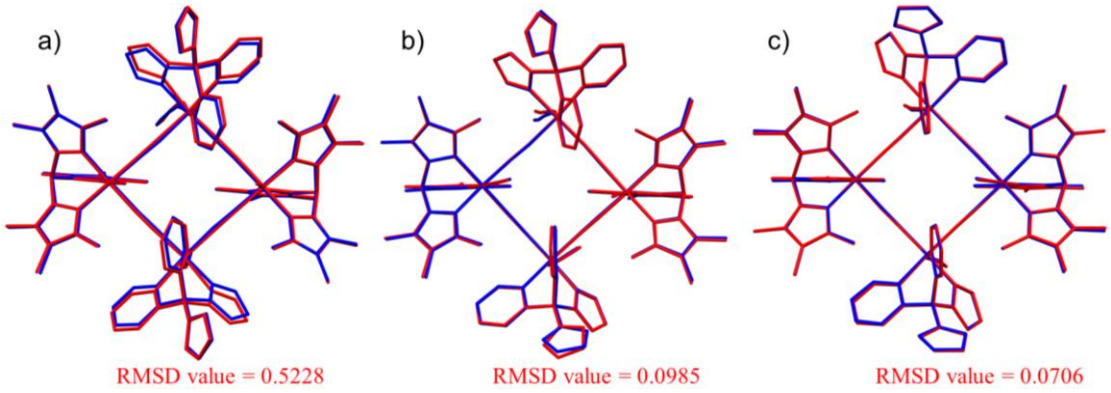

Figure S14. Molecule overlays of **1** at 300 and 100 K. Squares B (a), C (b), D (c) at 300 and 100 K are colored in red and blue, respectively.

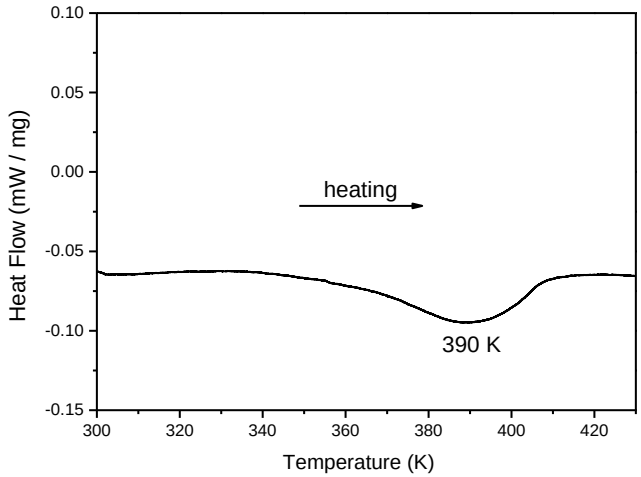

Figure S15. DSC plot of **1**·2Et_2O recorded at 300-430 K with a heating rate of 2 K/min.

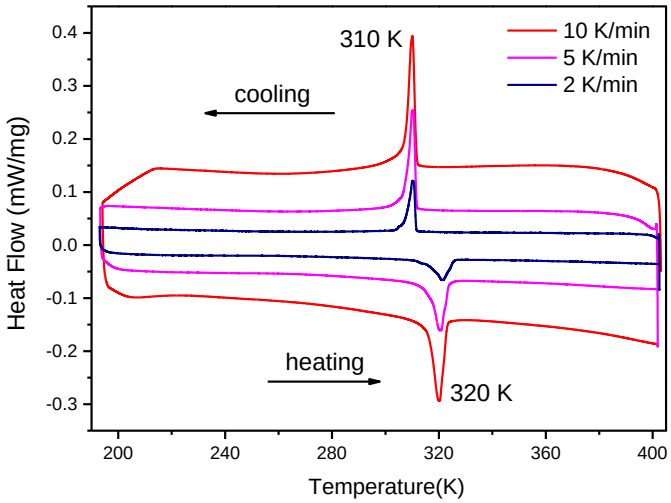

Figure S16. DSC plots of **1** recorded at 190-405 K with a scan rate of 10, 5 and 2 K/min, respectively.

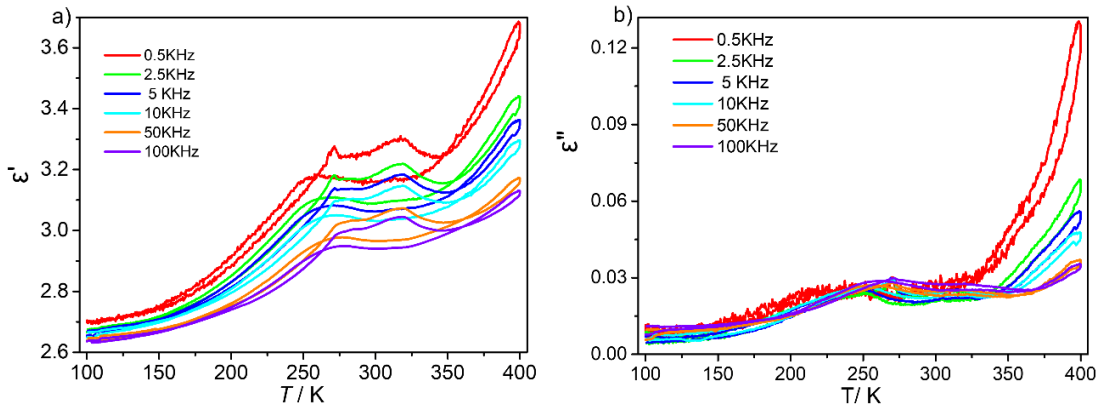

Figure S17. Temperature dependence of real (ε′) (a) and imaginary (ε″) (b) parts of dielectric function for **1** at different frequencies of 0.5, 2.5, 5, 10, 50 and 100 kHz in both heating and cooling modes from 100 to 400 K.